Characterisation of submarine depression trails driven by upslope migrating cyclic steps: Insights from the Ceará Basin (Brazil) / Maestrelli, D; Maselli, V; Kneller, B; Chiarella, D; Scarselli, N; Vannucchi, P; Jovane, L; Iacopini, D. - In: MARINE AND PETROLEUM GEOLOGY. - ISSN 0264-8172. - 115:(2020), pp. 104291-N/A. [10.1016/j.marpetgeo.2020.104291]

(Article begins on next page)

This paper has been submitted for publication to Marine Geology on 7 July 2018. Please note that subsequent version of this manuscript may have different content. Please feel free to contact any of the authors

Submarine depression trails driven by the interplay of density currents and fluid migration.

Maestrelli D.[1,2], Iacopini D.[3], Maselli V.[3], Chiarella, D.[4], Scarselli N.[4], Vannucchi P.[4,2], Jovane L.[5], Kneller B.[3]

[1]Consiglio Nazionale delle Ricerche, Istituto di Geoscienze e Georisorse (CNR-IGG), Via G. La Pira 4, Firenze, Italy

[2]Dipartimento di Scienze della Terra, Università di Pisa, Via S. Maria 53, 56126, Pisa, Italy

[3]Department of Geology and Petroleum Geology, University of Aberdeen, King's college, Aberdeen AB24 3DS, UK

[4]Department of Earth Sciences, Royal Holloway, University of London, Egham Hill, TW20, 0EX ,UK

[5]Instituto Oceanográfico, Universidade de São Paulo, Praça do Oceanográfico, 191, 05508-120, São Paulo, Brazil

Abstract

In this study, we propose a new depositional mechanism for the formation of sea floor depression features similar to pockmark trails, but generated by the interplay between turbidity currents and fluid migration. By using high-resolution 3D seismic data from offshore Ceará State (Brazil), we show how vertically stacked and upslope migrating sediment waves evolve into cyclic steps, promoting the formation of isolated sea floor depressions and, eventually, depression trails. Seismic interpretation and amplitude analysis indicate that the depression trails are very effective not only in shaping the submarine landscape and controlling sediment delivery to the basin but also in creating syn-depositional pathways for vertical fluid migration.

Keywords: sediment waves; fluid migration pathways; density currents; 3D seismic; Brazil

1. Introduction

The study of fluid migration and accumulation in marine sediments has attracted a large community of geoscientists due to their importance in predicting the presence of deep-seated hydrocarbon reservoirs and in understanding the seal capacity and the physical properties of specific stratigraphic intervals (Hovland, 2003). Trails of circular depressions with a preferred alignment have been observed in a number of different contexts, some in connection with vertical fluid migration. They have usually been described as being formed by dewatering of channel fill sands triggered by overpressure (i.e. pockmarks, Davies, 2003; Pilcher and Argent, 2007) or by turbidity currents that show streamwise alternations between sub- and super-critical flow regimes (Fildani et al., 2006; Covault et al., 2014). Heiniö and Davies (2009) described gravity-driven flows interacting with discontinuities in the topography of deep-sea channels. They showed that turbidity flows were able to trigger the formation of sediment waves that evolved into circular depressions, termed plunge pools, with no geophysical evidence of gas-charged sediments or fluid pipes. Vertically stacked circular depressions have also been observed in the late stage of infill of submarine canyons by Jobe et al. (2011). In this case, the troughs of a series of cyclic steps generated by dilute turbidity currents evolve into pockmark fields during the passive infill of the abandoned canyon (Jobe et al., 2011).

Here, we use high-resolution 3D seismic data from the offshore Ceará Basin (equatorial Brazil, Fig. 1) to describe a novel sedimentary feature generated by the interplay and mutual feedback between intermittent fluid flow and long-lasting conditions of sediment supply from turbidity currents. The results obtained will be discussed in the light of better understanding the processes controlling the evolution of the Brazilian margin but also to presenting a new mechanisms responsible of the formation of the sea floor topography.

2. Regional geology and study area

The South Atlantic rift system developed in the Mesozoic time due to the breakup of the Gondwana super-continent (Morihak et al., 2000) and is limited to the north by transcurrent fault systems associated with oceanic fracture zones (the Romanche Fracture Zone, RFZ in Fig. 1) and to the south by fracture zones in the Malvinas (Falkland) Plateau (MP in Fig.1). The area of interest is considered part of the Brazilian equatorial margin (Jovine et al, 2016) which opening occurred during the Early Cretaceous (Neocomian– Barremian; Asmus and Porto, 1972). However due to the presence of a wide magnetic quiet zone (constant magnetic polarity) from early Aptian to Campanian times, reconstruction of plate motion during the early drift stage, and the continent-ocean boundary location are still subjects of a long-lasting debate (Chang et al., 1992).

The study area is located in the pull-apart Meso-Cenozoic Ceará Basin in the northern Brazilian Equatorial passive margin (Fig. 1). Ceará Basin -offshore covers a combined area of approximately 105,000 km^2 and forms the southern flank of the RFZ. The RFZ is a linear fracture zone with an average width of approximately 16 km that extends over 4500 km from offshore northern equatorial Brazil to its conjugate margin near offshore Ghana and Togo/Benin. From a tectonic point of view, the Ceará Basin has three stages of evolution: rift (Neocamian–Eo–Aptian), post-rift (Neoaptian–Eo–Albian), and continental drift (Albian–Holocene) stages. The rift, post-rift, and continental drift stages are characterised by continental, transitional, and marine mega-sequence deposits, respectively (Matos, 1992). The study area extends into the Mondaú sub-basin, part of the Ceará

Basin, close to the junction with the Potiguar Basin (Fig. 1). The seafloor lies at about 100 metres water depth at the shelf edge, dropping to more than 2000 metres toward the continental rise, with a change of gradient from 1° to more than 3° downslope. Due to the lack of well data, the Neogene stratigraphy is still pretty elusive. Using our seismic dataset the Neogene stratigraphy can be subdivided into two main units (Fig. 2): (i) an upper unit (above H1) characterized by a series of canyons acting as well-developed sediment bypass systems, and (ii) a lower unit (below H1) characterized by amalgamated channel systems, locally interbedded with mass transport deposits. From offshore well data (CES-112, Fig. 1) through regional 2D seismic line correlations, the base of the lower unit has been dated as post upper-Miocene (Jovine et al., 2016).

From an oceanographic point of view, the area is characterized by trade winds in the E–NE direction, with maximum velocity up to 18 m/s (Vital et al., 2010). The North Brazilian Current flows in a W–NW direction relatively parallel to the coast (Vital et al., 2010; De Almeida et al., 2015). The bottom currents, which attain velocities of 30–40 cm/s on the shelf, are overlain by tidal and wave components that are pretty important in triggering shallow low density current (Knoppers et al., 1999; Vital, 2009).

3. Dataset and Methods

The dataset from the Ceará Basin consists of a high-quality 3D full stack, Kirchhoff time migrated reflection seismic volume of ~1600 km^2 acquired by PGS in 2009 (Fig. 1). The line spacing is 12.5 m in both in-line and cross-line directions. The sample interval is 2 ms (milliseconds). The data are zero-phase migrated and displayed with Society for Exploration Geologists (SEG) normal polarity, so that an increase in acoustic impedance is represented by a blue-red-blue reflection loop. The dominant frequency of the section of interest ranges between 30 and 50 Hz with a vertical resolution of ca.

10-18 meters. Velocity values of 1500 ms^{-1} have been used for seawater and 1800 to 2500 ms^{-1} for the studied interval from the nearest (2 km to the SE) well CE-112 (Fig. 1; Conde et al., 2007). Structural maps of key horizons were generated from a subset of the data (seabed in Fig. 1, Fig. 3), using a combination of two seismic attributes (root mean square of amplitude, and variance; Chopra & Marfurt, 2007). Finally, a qualitative amplitude versus offset (AVO) analysis (Castagna et al. ,1998) using partial stack data imaging a portion of the seismic area has been applied to investigate the significance of some of the bright and weak anomalies affecting the depression trails . The partial stacks have been processed following a robust workflow for amplitude preservation and noise suppression (see supplementary material).

4. Results: sedimentary architectures and amplitude anomalies

4.1. Sedimentary architecture

In the upper slope region of the study area, the sea floor is characterized by fields of sediment waves (SW) with an upslope direction of migration, showing a wavelength of about 250 meters and a height of 10-50 metres (Fig. 2a, and Fig. 4). The sediment waves evolve downslope into circular to elliptical depressions with a maximum diameter of 1 km (Figs. 1 and 4), maximum depth of 300 m with asymmetric internal flanks (Figs. 2a, c). These depressions occur either isolated, recalling the geometry of pockmarks (arrow 1 in Fig. 2b, Fig. 4), or in trails aligned downslope and often merging together (arrow 2, Fig. 2b), developing a more elongated (channel-like) composite morphology (arrow 3 in Fig. 2b, Fig. 4). Seismic reflection profiles reveal that in the subsurface (Fig. 2) these features develop as a series of vertically-stacked concave-up units, characterized by variable amplitude. These concave-up structures represent the troughs of vertically stacked depressions (Fig. 2a) and are characterized by minor erosional surfaces (red dotted line, Fig. 2b) and truncated reflections (arrow 2 in Fig. 2b), bounded by continuous horizons (H2, H3, Fig. 2d). In plan view, the vertically stacked concave-up structures highlighted in Figure 2b appear as sub-circular features (green arrow in Fig. 3), but also isolated depressions (Fig. 4). Some of these features extend from the basal horizon (H2) up to the sea floor, maintaining almost the same position and finally appearing as a depression on the seabed (Fig. 2c). Other examples are filled by sub-horizontal units that onlap the concave-upwards bounding surface, leaving them with no expression on the seafloor (Fig 2d). Mapped seismic horizons (named H1 to H3 from deep to shallow, Fig. 3) across the Neogene units reveal the following key information: a) embryonic channel features observed in H1 (Fig. 3) representing the precursors to the main active channels currently observed on the seafloor (SB in Fig. 3); b) the mapped seismic horizons H1 to H3 (Fig. 3) show that the embryonic channel consistently behaved as an erosion-prone feature through time, while the inter-channel aggraded continuously; c) both isolated depressions and linear arrays of depressions are observed across the entire area, along the channel and beyond along the inter-channel (H1-H3 in Fig. 3). The recently active channel has deep erosive walls, 200-300 meters high, with little or no evidence of overspill deposit (Fig. 4).

At a closer scale of observation (Figs. 2b, d), stacking of concave reflections shows that they develop as a set of aggrading packages, with the troughs of each package displaced either sub-vertically or upslope from the previous one (Figs. 2c, d). Each package is commonly separated from the following one by a draping unit (when not eroded) observed inside the depression (Figs. 2b, c). Furthermore, horizons H1, H2 and H3 can be traced in the entire dataset and probably originated during periods of reduced turbidity current activity and increased pelagic/hemipelagic deposition draping both depressions and abandoned canyons (green arrow in H3, Fig. 3). While at the seabed and in the subsurface some of the depression trails appear isolated, many others are localized along the axis of the canyon, resulting in a stepped pattern evident in both buried and active canyons (Figs. 2c and

3 H1 to SB). Finally, the most notable feature is the correspondence between the centres of the depressions and the brightness of some reflectors within them (localised positive and negative weak to bright amplitude anomalies) as shown in figures 2b, c and d.

4.2. Amplitude anomalies across trough structures:

In the studied dataset, there is a clear correspondence between stacked positive bright amplitudes (arrows 1 and 3 in Fig. 2b), negative bright amplitude (arrows 4 and 5 in Fig. 2c), and depressions (arrows in Figs. 2b to d). Several troughs are also characterized by the presence of a flat spot (see arrows 9 and 10 above H3, Fig. 3c) lying inside the buried depressions within the passive infill of the depressions. In detail, the amplitude brightness within the trough structures (Figs. 2b, c and d) indicates the following trend:

- In Figure 2b, stacked positive anomalies with weaker amplitude than the seabed are observed through the fill of the trough from bottom to top (arrows 1 and 2). In some cases, clear flat spot (arrows 3) with a concordant polarity to the seabed appear in the apparently passive infill.
- In Figure 2c, we observe clear depressions onto the seafloor, both affected by weak to strong (arrow 5) negative anomalies.
- In Figure 2d, weak bright anomalies with contrasting polarity to the seabed (arrows 8 and 9) are observed also across the aggrading trough. Arrows 6 and 10 shows soft flat spots within the infill. Between trough trails, by contrast, strong negative bright spots are present (arrow 7).

AVO analysis, performed using partial stack imaging of some of the flat spots (Figs. 5a and c) and plotted in gradient versus reflectivity (intercept) diagram (Fig. 5b) indicates that the weak positive amplitude anomalies (observed distributed across the depression trails, Fig 5c) show a lateral spread (green triangle) along the background distribution but with a weak change in fluid saturation or shale content (as indicated by the red arrows in Fig 5b). We do not observe any clear distinctive trend toward the negative reflectivity and negative gradient quadrant.

5. Discussion: a model for the depression trails and fluid migration pathways

5.1. Amplitude anomalies and trough structures

In seismic reflection data, isolated bright spots (regardless of the polarity) commonly suggest a change in the grain size or cementation of the sediment, and/or the presence of fluid with properties significantly different from normal saline pore water (Asveth et al., 2013; and references therein). Below the seabed, where sand is poorly consolidated, the negative amplitude anomalies may well indicate presence of gas fluid (Asveth et al., 2013). On the other hand, weak positive amplitude anomalies affecting the troughs (Fig. 2c) are more ambiguous and cannot be unequivocally associated with fluid (Asveth et al., 2013) but rather to either sediment cementation or grain size changes.

The plotted AVO analysis (see supplementary material) in a diagram gradient versus intercept (Fig. 5) confirms the ambiguity of those anomalies, as no clear distribution trend (versus the lower or both negative gradient and intercept quadrant of the diagram) typical of gas fluid is observed. The green points clearly distribute and scatter along the main diagonal brine sand background with no or a minimal deviation respect to it (Fig. 5b).

In particular, these stacked weak amplitude anomalies at the concave base of the structures may instead suggest:

a) Vertical variation of grain size and cementation (and consequently porosity and permeability) within the troughs of these depressions (weak positive anomalies, Figs. 2b and d);
b) Fluid presence within the vertically stacked depression, perhaps facilitated by their petrophysical characteristics (increased porosity and permeability), (negative amplitude anomalies, Fig. 2c).

Field evidences from different depositional settings prove the importance of unidirectional flows – both bottom currents and subsurface fluid migration – in the reorganization of surface and subsurface sediments (Gong et al., 2012). Accumulation of coarse-grained and porous sediment related to the vertical aggradation of consecutive depressions may explain both the weak positive amplitude anomalies produced by variation of porosity/granulometry and preferential cementation along the trough of the depressions (Fig. 2d). In areas saturated by fluid such grain size variation might also promote and localize preferential pathways for fluid migration (Fig. 2c). The bright negative amplitude anomalies observed all along the troughs in Figure 2c (arrows 4 and 5) might indeed represent active fluid pathways exploiting the concave depression structure all the way up to the seabed. However, following the above considerations figures 2b and 2d seem to suggest that the positive amplitudes across the troughs (arrows 1 to 3) are expressions solely of grain-size variations and cementation effects.

5.2. Down-slope arrays that nucleated the 'canyons'

Following the all previous observations, we infer that the extensive field of circular depressions was initiated (H1, green reflector in Figs. 2 and 3) as a series of sediment waves (SW in Fig. 2a) related to periodic instabilities generated by unconfined and low density gravity currents (LDGf in Fig. 2a;

arrow 4 in Fig. 2; green arrows in Fig. 4; Lesshafft et al., 2011), commonly generated by the impact of storm waves on the outer shelf and upper slope (Mulder et al., 2001; Puig et al., 2004;). These may interact with span-wise instabilities (Hall et al., 2008) to generate the observed randomly distributed depressions on the slope (Fig. 2 S1, Fig. 3 H1), and led to coalescence of some of these depressions into systematic downslope arrays (Fig. 2, arrows 2 and 3). These appear to have been amplified and perpetuated as cyclic steps (Cartigny et al., 2011; CS in Fig. 2a and 4), features that have been recognized in many submarine canyons and channel systems (Normark et al., 2002; Symons et al., 2016).

The conceptual diagram in Figure 6 presents an evolutionary sequence for these shallow structures. Each depression evolves in two more or less distinct stages.

(a) Preferential sea-floor erosion (truncation of seismic reflectors) amplifying the depressions (Fig. 6, T1);
(b) Partial fill of the depression, shown by onlapping seismic reflectors of varying amplitude, and with geometries ranging from planar and horizontal with abrupt onlap (Fig. 2b, arrows 2 and 3) to concave-upwards with only slight thickening into the base of the depression (Fig. 2b, arrow 1; Fig. 2c arrows 4 and 5, Fig. 6, T2 to T3).

We relate sea-floor erosion to the formation of cyclic steps (clearly visible in figures 2a and 3) by bypassing of turbidity currents along the pathways created by coalesced depressions. The more isolated depressions experienced less (if any) erosion (Figs. 2c and 3, SB), being off the main fairway. Flat, high-amplitude fill is found within the continuous downslope arrays of depressions, and thus occurs in areas of prior erosion which, we surmise, is an indication of more energetic and perhaps coarser-grained and higher-density turbidity currents (e.g. Talling et al., 2012). In contrast, the concave-upwards fills, which tend to show only relatively slight thickening into the depression, suggests lower density, finer-grained turbidity currents, moving downslope away from the main sediment fairway. These interpretations are consistent with our interpretation of the amplitudes.

5.3. Depression trail and fluid pathway

A detailed analysis of the seismic amplitude across the entire sequence clearly shows that the concave up fills of both isolated troughs and depression trails are affected by weak to bright amplitude anomalies from bottom to top. In some cases (Fig. 2c) the concave-upward fills (with slight thickening into the depressions) show weak to strong negative anomalies suggesting the presence of fluid affecting the trough. In other cases (Fig. 2d), flat high amplitude fills can be observed along the depression trail. The negative amplitude indicates the presence of fluid either still sealed by the draping unit (arrows 9 and 10 in Fig. 2d) or leaking to the surface (arrow 4 in Fig. 2d); while the positive amplitude may suggest a grain size or cementation effect (footprint of past fluid deposition). In both cases, the bright anomalies within the troughs may either represent the presence of (or a pathway for) fluid, or the presence of coarser grained sediment. Finally, the clear onlapping nature of the main bright infill and flat spot onto the erosive surface suggests that fluid may have migrated and/or been trapped during the cyclic erosional and depositional evolution of the trough. This allows us to infer that the depression trails may have acted as preferential pathways for syn-depositional vertical fluid migration. Therefore the evolution of the depression trails might include a punctuated interaction between turbidity currents and fluid flow to the sea-floor, generating re-suspension of fine sediments, producing a passive enrichment in coarser fractions during the upslope migration and stacking of the troughs of these cyclic steps (Fig. 4 T2 to T3).

6. Conclusions

We describe a dispersed distribution of seafloor depressions that resemble classical pockmarks. Their internal architecture and reflection configuration support the hypothesis that these trails of depressions are generated by upslope migrating cyclic steps produced by gravity-driven flows. Amplitude analysis across the depression trails indicates that fluids may exploit pathways generated by the troughs of these vertically stacked depressions or cyclic steps. The interaction between turbidity currents and fluid flow might generate re-suspension of fine sediments, producing a passive enrichment in coarser fractions and the upslope migration and stacking of the troughs of these features. Our observations suggest that the interplay between slope sedimentation and fluid flow may represent a key process in shaping the seafloor of many slope settings worldwide.

Acknowledgments

We sincerely thank Petroleum Geo-Services (PGS), CGG and specifically David Hajovsky and C. Baron who kindly furnished the dataset and allowed us to show these results. We are grateful to Huuse, Duarte for their constructive comments of a previous draft. D.M. was funded through the Tuscany PhD Regional program [grant POR ICO FSE 2014/2020-Asse C] and the Erasmus+ exchange for his visit in Aberdeen.

Declaration of interest

Declarations of interest: none.

References

Almeida, N.M. Vital, H.,Gomes, M.P. 2015. Morphology of submarine canyons along the continental margin of the Potuigar Basin , NE Brazil. Marine and Petroleum Geology 68, 307-324

Asmus, H.E. , Porto R. 1972. Classification of Brazilian sedimentary basins according to plate tectonics. Congresso Brasileiro de Geologia 26, Belém (Ed.), Anais do XXVI Congresso Brasileiro de Geologia, 2, Sociedade Brasileira de Geologia, São Paulo (1972), pp. 67-90. (in Portuguese).

Avseth,P., Mukerji, T. and Mavko G. 2005. Quantitative seismic interpretation. Cambridge Press.

Cartigny, M.B., Postma, G., van den Berg, J.H., and Mastbergen, D.R., 2011. A comparative study of sediment waves and cyclic steps based on geometries, internal structure and numerical modelling. Marine Geology 280, 40-56. https://doi.org/10.1016/j.margeo.2010.11.006

Cartwright J. and Santamarina, C., 2015. Seismic characteristics of fluid escape pipes in sedimentary basins: Implications for pipe genesis. Marine and Petroleum Geology, 65, 126-140. https://doi.org/10.1016/j.marpetgeo.2015.03.023

J.P. Castagna, H.W. Swan, D.J. Foster. Framework for AVO gradient and intercept interpretation. 1998. Geophysics, 63, 948-956.

Chang, H.K., R. O. Kowsmann, A. M. F. Figueiredo, and A. A. Bender, 1992. Tectonic and stratigraphy of the East Brazil Rift system: an overview. Tectonophysics, 213, 97-138.

Covault, J.A., Kostic, S., Paull, C.K., Ryan, H.F., Fildani, A., 2014. Submarine channel initiation, filling and maintenance from sea-floor geomorphology and morphodynamic modelling of cyclic steps. Sedimentology 61, 1031-1054.

Davies, R. J., 2003. Kilometer-scale fluidization structures formed during early burial of a deep-water slope channel on the Niger Delta. Geology, 31-11, 949-952. https://doi.org/10.1130/G19835.1

Gong, C., Wang, Y., Peng, X., Li, W., Qiu, Y., and Xu, S., 2012. Sediment waves on the South China Sea Slope off southern Taiwan: Implications for the intrusion of the Northern Pacific Deep Water into the South China Sea. Marine and Petroleum Geology 32, 95-109. https://doi.org/10.1016/j.marpetgeo.2011.12.005

Hall, B., Meiburg, E. and Kneller, B., 2008. Channel formation by turbidity currents: Navier–Stokes-based linear stability analysis. *Journal of Fluid Mechanics*, *615*, pp.185-210.

Heiniö, P., and Davies, R.J., 2009. Trails of depressions and sediment waves along submarine channels on the continental margin of Espirito Santo Basin, Brazil. Geological Society of America Bulletin 121, 698-711. https://doi.org/10.1130/B26190.1

Ho, S., Cartwright, J., and Imbert, P., 2012. The Formation of advancing pockmarks arrays: an interplay between hydrocarbon leakage and slope sedimentation. AAPG Annual Convention and Exhibition, Long Beach California, April 22-25.

Hovland, M., 2003. Geomorphological, geophysical, and geochemical evidence of fluid flow through the seabed. J. Geochem. Exploration, 78-79, 287-291

Jobe, Z. R., Lowe, D. R., and Uchytil, S. J., 2011. Two fundamentally different types of submarine canyons along the continental margin of Equatorial Guinea. Marine and Petroleum Geology, 28(3), 843-860. https://doi.org/10.1016/j.marpetgeo.2010.07.012

Judd, A., and Hovland, M., 2009. Seabed fluid flow: the impact on geology, biology and the marine environment. Cambridge University Press. New York, 492 pp

Knoppers, B., Ekau, W., Figueiredo, A.G., 1999. The coast and shelf of east and northeast Brazil and material transport. Geo Mar. Lett., 19, pp. 171-178

Lesshafft, L., Hall, B., Meiburg, E. and Kneller, B., 2011. Deep-water sediment wave formation: linear stability analysis of coupled flow/bed interaction. Journal of Fluid Mechanics, 680, pp.435-458.

Matos, R.M.D., 2000. Tectonic evolution of the equatorial South Atlantic. W.U. Mohriak, M. Talwani (Eds.), Atlantic Rifts and Continental Margins, Geophysical Monograph, 115, American Geophysical Union . 331-354

Mohriak, W.U., M. Basseto, and I.S Vieira, 2000. Tectonic Evolution of the Rifted Basins in the Northeastern Brazilian Region. In: W.Mohriak and M.Talwani, eds., Atlantic Rifts and Continental Margins: Geophysical Monograph 115, 293-315.

Mulder, T., Weber, O., Anschutz, P., Jorissen, F., and Jouanneau, J.M., 2001. A few months-old storm-generated turbidite deposited in the Capbreton Canyon (Bay of Biscay, SW France). Geo-Marine Letters, 21(3), 149-156. doi:10.1007/s003670100077

Normark, W.R., Piper, D.J., Posamentier, H., Pirmez, C., and Migeon, S., 2002. Variability in form and growth of sediment waves on turbidite channel levees. Marine Geology 192, 23-58. https://doi.org/10.1016/S0025-3227(02)00548-0

Osborne, M. J., and Swarbrick, R. E., 1997. Mechanisms for generating overpressure in sedimentary basins: a reevaluation. AAPG bulletin, 81(6), 1023-1041.

Pilcher, R., and Argent, J., 2007. Mega-pockmarks and linear pockmark trains on the West African continental margin. Marine Geology 244, 15-32.

Puig, P., Ogston, A. S., Mullenbach, B. L., Nittrouer, C. A., Parsons, J. D., and Sternberg, R. W., 2004. Storm-induced sediment gravity flows at the head of the Eel submarine canyon, northern California margin. Journal of Geophysical Research: Oceans, 109(C3). doi:10.1029/2003JC001918.

Szatmari, P. , Françolin, J.B.L. , Zanotto, O., Wolff, S. 1987. Tectonic evolution of the Brazilian equatorial margin Rev. Bras. Geociênc., 17, 180-188. (in Portuguese)

Symons, W. O., Sumner, E. J., Talling, P. J., Cartigny, M. J., and Clare, M. A., 2016. Large-scale sediment waves and scours on the modern seafloor and their implications for the prevalence of supercritical flows. Marine Geology, 371, 130-148. https://doi.org/10.1016/j.margeo.2015.11.009

Talling, P.J., Masson, D.G., Sumner, E.J. and Malgesini, G., 2012. Subaqueous sediment density flows: Depositional processes and deposit types. Sedimentology,59, 1937-2003.

Vital, H. 2009. The mesotidal barriers of Rio Grande do Norte. S. Dillemburg, P. Hesp (Eds.), Geology of Brazilian Holocene Coastal Barriers, Springer-Verlag, Heidelberg, pp. 289-324

Vital, H. Gomes, M.P., Tabosa, W.F.,Frazao, E.P, Santos, C.L.A., Placido Junior. J.S. 2010. Characterization of the Brazilian Continental shelf adjacent to Rio Grande do Norte State, NE Brazil. Braz. J. Oceanogr., 58, 43-54

Figure captions

Figure 1. The study area, offshore of Ceará state (Brazil). The white polygon represents the dataset, while the red rectangle marks the area from where examples shown in this paper come. The blue surface represents the fully mapped seabed. Arrow 1: isolated pockmark-like structure; Arrow 2: depression trails aligned parallel to the sea floor gradient; Arrow 3: elongated channel-like morphology; Arrow 4: roughness of the paleo-sea floor triggered by the impact of storm waves.

Figure 2. (a) 3D seismic block showing the depressions at the seabed, the turbidite channel and the smaller canyons. Inside this latter are visible depressions-stepped pattern, generated by sediment waves (SW) and cyclic steps (CS). LDGf: Low Density Gravity flow; FM: Fluid Migration. (b) A crossline (A-B) showing stacked depressions culminating in pockmark-shaped depressions at the seafloor. (c) Stacked bright soft anomalies (Arrows 4 and 5) affecting two main depressions both emerging on the seafloor. (d) Section CD (inline) showing buried stacked depressions. Arrows 6 and 9 represents soft (negative) amplitude bright anomalies (arrow 9 as a flat spot). Arrows 7 and 10 shows weak to hard anomalies concordant with the seafloor. Seismic section traces are reported in Figure 3 (H3). Red arrows in b, c and d indicate bright anomalies across the trough.

Figure 3. The mapped key horizons H1, H2, H3 and the seabed (SB). Yellow boundaries highlight the position of the turbidite channels. Section AB, CD and EF represent the images shown in Figure 2.

Figure 4. Portion of the mapped seabed highlighting the presence of canyons, turbidite channels and widely distributed pockmark-shaped depressions. LDGf: Low Density Gravity flow; HDGf: High Density Gravity flow

Figure 5: AVO analysis using partial stack from a section of the investigation area. (a) Location of the 3D seismic dataset (CGG Ceara basin, partial stack) , Ceara basin. (b) Gradient versus intercept crossplot of the amplitude selected from Figure 5c. In blue triangle are the normal amplitude brine sand defining the background trend. In green, the weak positive bright green amplitude selected from Figure 5c. Notice the poor/weak fluid factor effect suggesting a non-hydrocarbon effect in controlling the brightness. It indicates that the weak positive amplitude anomalies observed across the depression trails do shows a possible changes in fluid saturation or shale content but with no regard to the typical gas or hydrocarbon anomaly AVO classes (Avseth et al.,2005). (c) Seismic section showing the selected area under analysis: in green the weak brightness from the depression trough; in blue the sand.

Figure 6. Schematic sketch illustrating a possible evolution of stacked sediment waves, migrating upslope and creating a permeable preferential path for upward fluid flow. See text for explanation. Acronyms as in Figure 2.

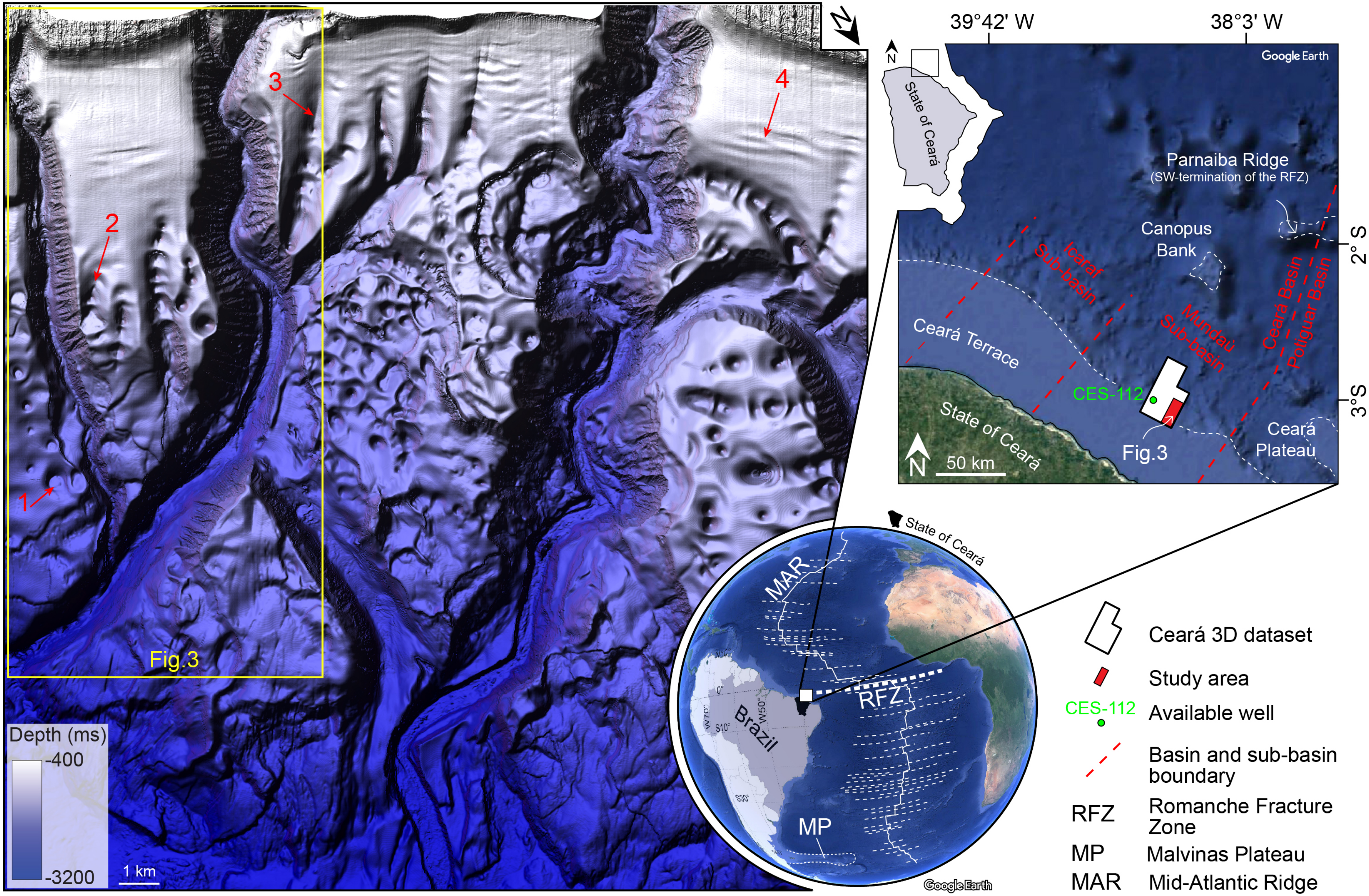

3
4
2
1
Fig.3
Depth (ms)
-400
-3200
1 km
39°42' W
38°3' W
Google Earth
N
State of Ceará
Parnaiba Ridge
(SW-termination of the RFZ)
Canopus Bank
Icaraí Sub-basin
Mundaú Sub-basin
Ceará Basin
Potiguar Basin
Ceará Terrace
CES-112
Fig.3
Ceará Plateau
State of Ceará
50 km
2°S
3°S
State of Ceará
MAR
RFZ
Brazil
MP
Ceará 3D dataset
Study area
CES-112
Available well
Basin and sub-basin boundary
RFZ
Romanche Fracture Zone
MP
Malvinas Plateau
MAR
Mid-Atlantic Ridge

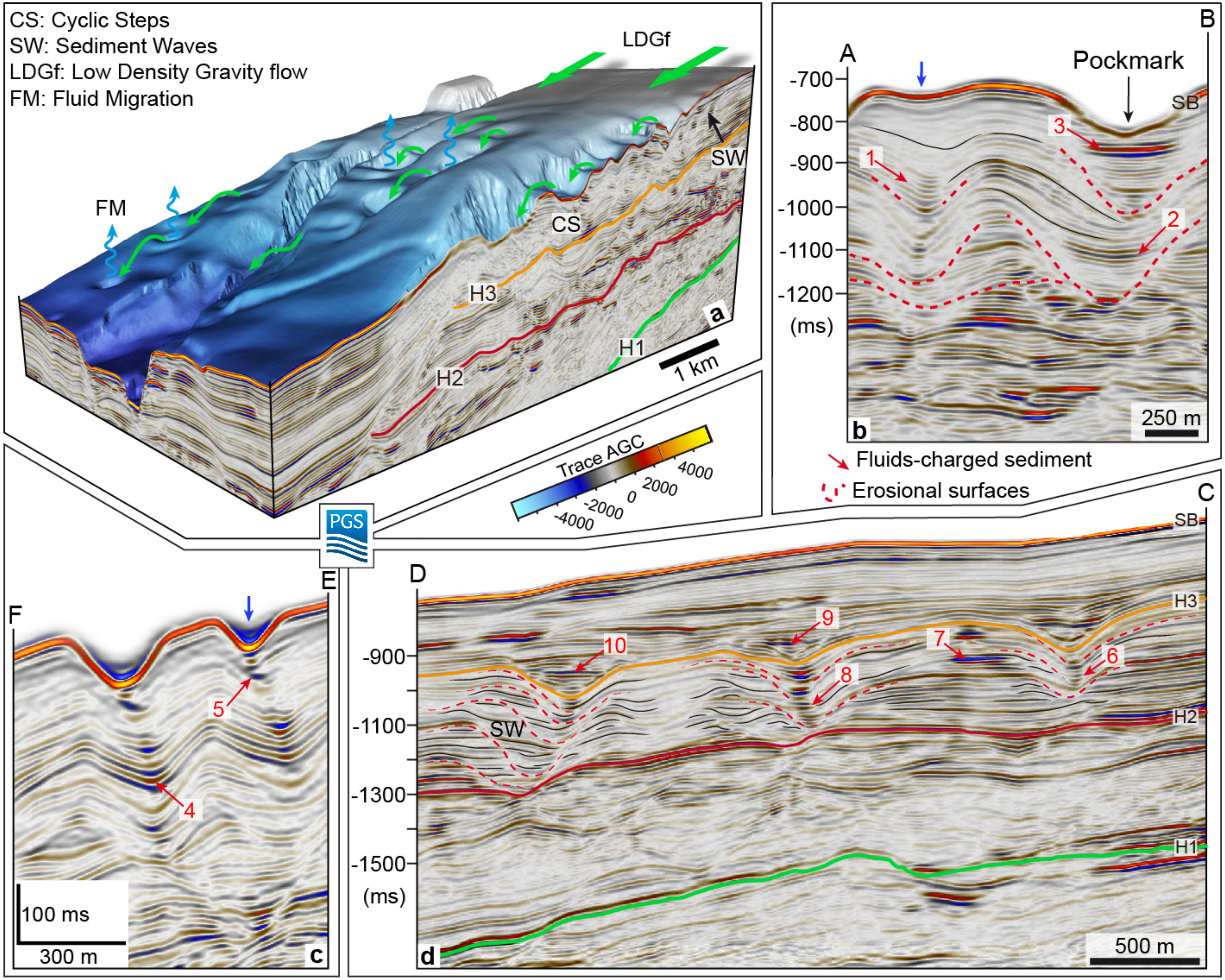

CS: Cyclic Steps
SW: Sediment Waves
LDGf: Low Density Gravity flow
FM: Fluid Migration
LDGf
SW
CS
FM
H3
H2
H1
1 km
a
Trace AGC
-4000
-2000
0
2000
4000
PGS
A
B
Pockmark
SB
-700
-800
-900
-1000
-1100
-1200
(ms)
1
2
3
250 m
b
Fluids-charged sediment
Erosional surfaces
F
E
5
4
100 ms
300 m
c
D
C
SB
H3
H2
H1
10
9
8
7
6
SW
-900
-1100
-1300
-1500
(ms)
500 m
d

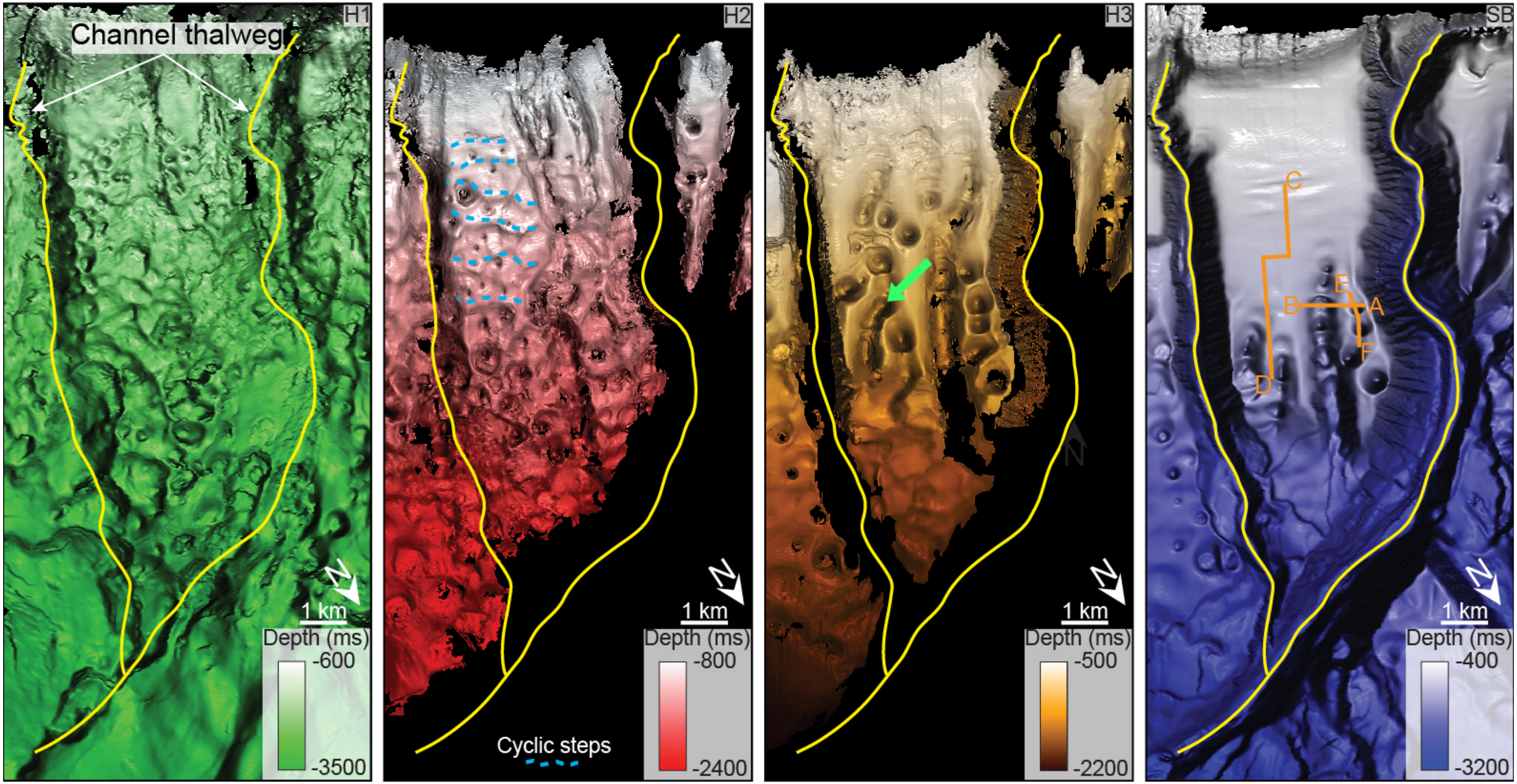
H1
Channel thalweg
1 km
Depth (ms)
-600
-3500
H2
1 km
Depth (ms)
-800
-2400
Cyclic steps
H3
1 km
Depth (ms)
-500
-2200
SB
C
B
E
A
F
D
1 km
Depth (ms)
-400
-3200

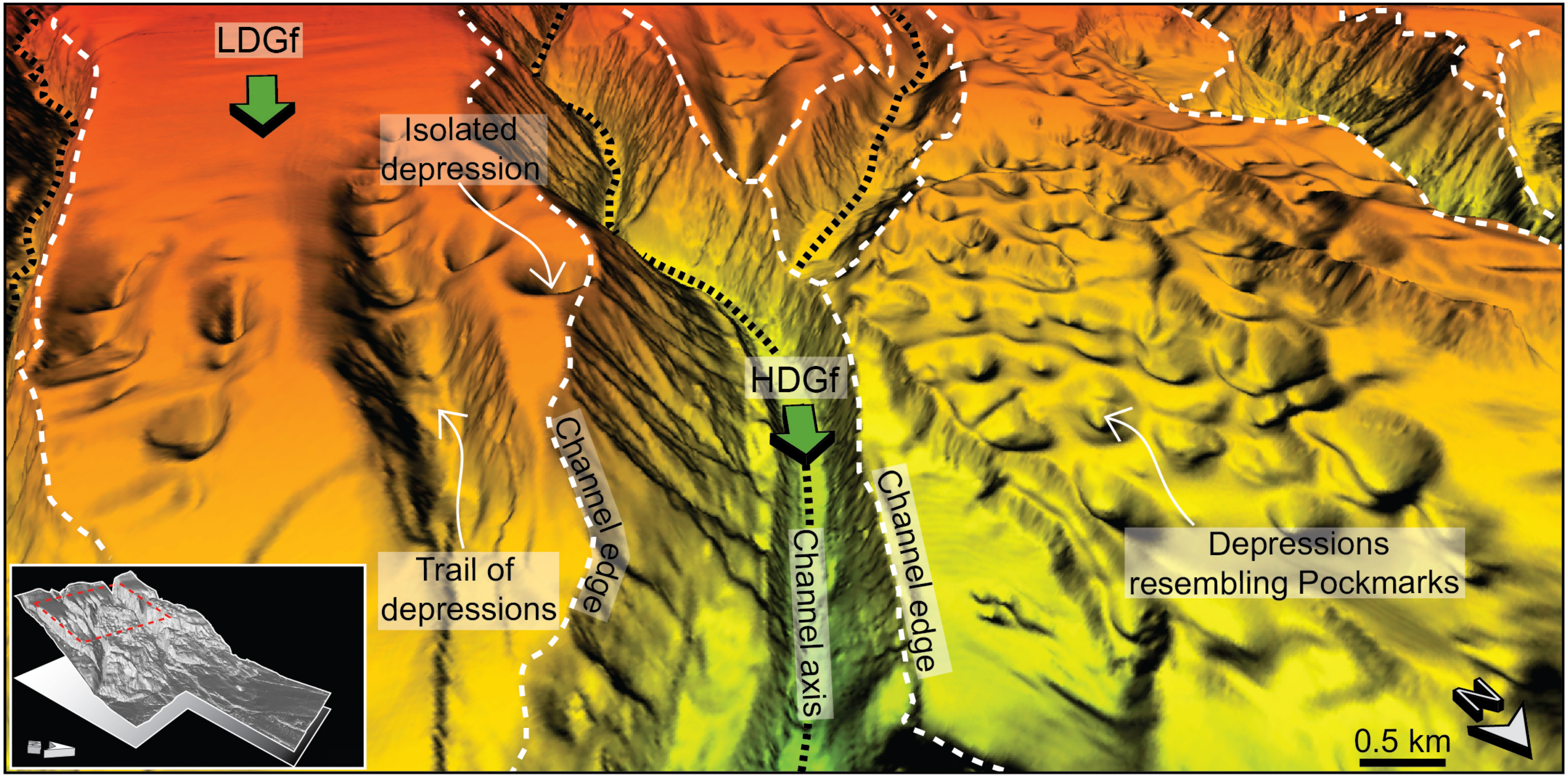
LDGf
Isolated depression
Trail of depressions
Channel edge
HDGf
Channel axis
Channel edge
Depressions resembling Pockmarks
N
0.5 km

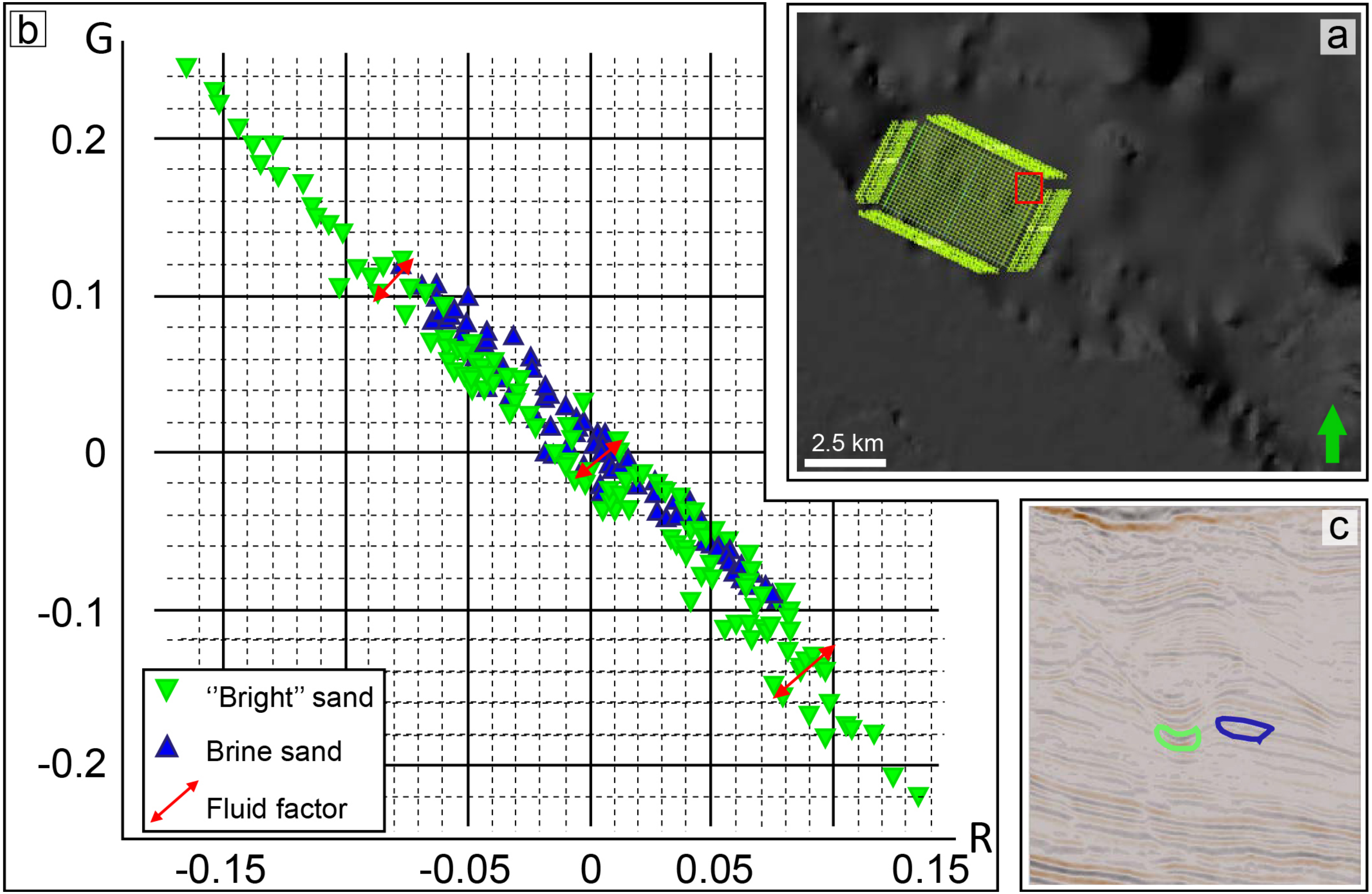

b
G
R
0.2
0.1
0
-0.1
-0.2
-0.15
-0.05
0
0.05
0.15
"Bright" sand
Brine sand
Fluid factor
a
2.5 km
c

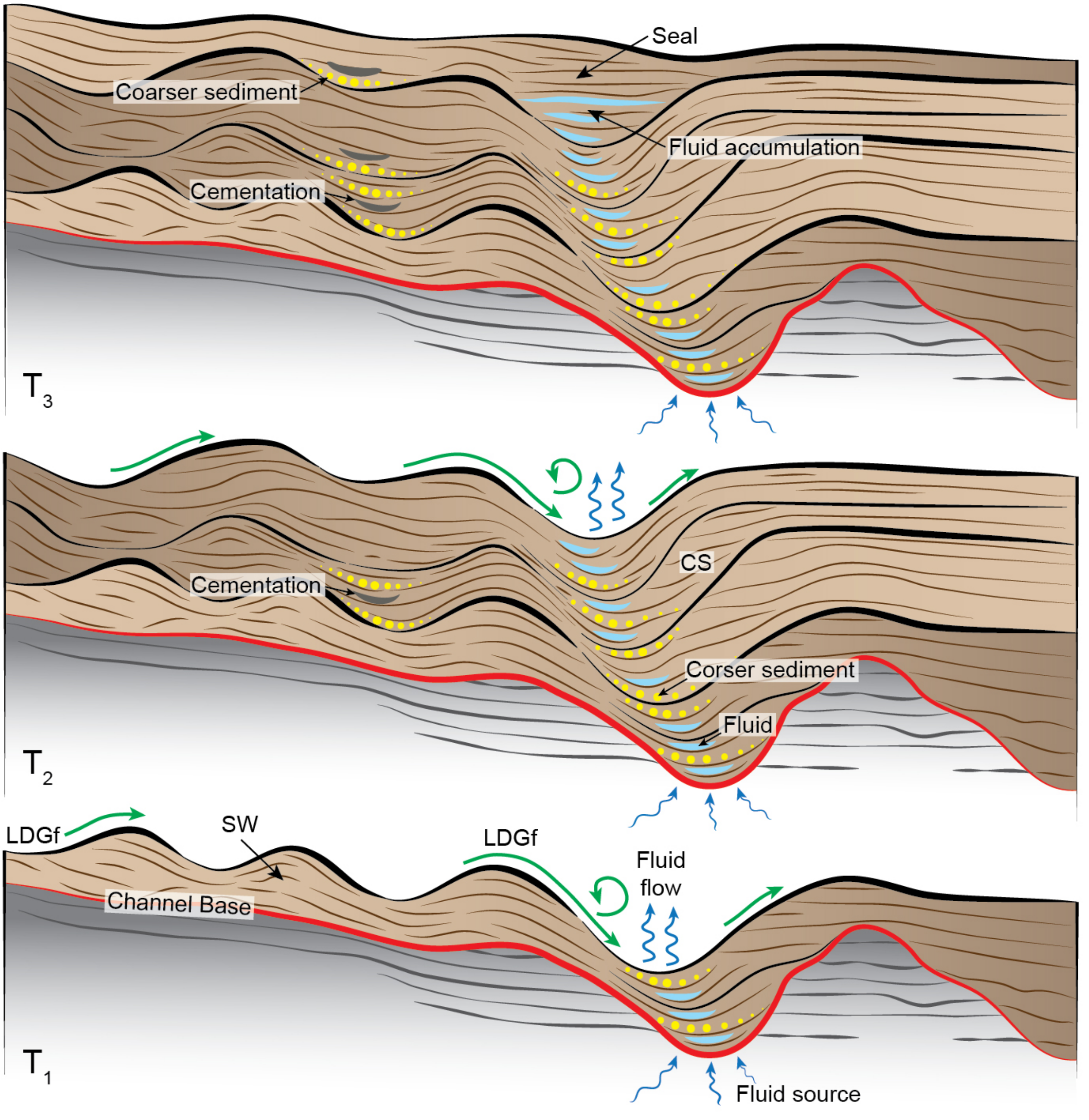

Seal
Coarser sediment
Fluid accumulation
Cementation
T3
Cementation
CS
Corser sediment
Fluid
T2
LDGf
SW
LDGf
Fluid flow
Channel Base
T1
Fluid source

Supplementary material

AVO using partial stack.

Partial stacked data provided by CGG have been used to explore some qualitative amplitude analysis in the area of interest. The partial stack data processed and released by CGG (Fig. 1) is characterized by near middle and far reprocessed stack data. The data have been processed using an amplitude preservation processing that included geometric spreading corrections and preserved amplitude pre-stack time migration (PSTM). The character of the wavelet discovered during the well analysis was used to correct the Near stack to zero phase. In order to use pre stack data for amplitude versus offset analysis a seismic data condition workflow was necessary to reduce the Noise in the P wave in the form of wavelet variation and the residual NMO biased information.

Seismic data conditioning workflow:

The following steps were key to the analysis:

- Phase differences: this is produced by generating peak and through volumes and comparing them and minimizing the difference. The phase was corrected by designing and applying matching filters to match the far stack to the near stack.
- Bedform stack analysis: a bedform indicator attributes for each partial stack groups was applied and then combined
- Frequency changes : instantaneous frequency were calculate for the partial stack volume and compared using the following algorithm :

  (((im1>0)&(im2>0))*(im2-im1))

  Where im1 and im2 represent the two main partial stack volumes in analysis

- A Time Alignment – time shifts misalignments are corrected.

As an initial test, a small subset was extracted from the partial stacks for testing of different Seismic Data Conditioning algorithm and the seismic data conditioning workflow was applied to correct for phase, frequency, amplitude and time differences. Once the exact procedure was outlined and tested, the workflow was applied and reviewed throughout the entire volume

Seismic data conditioning scheme

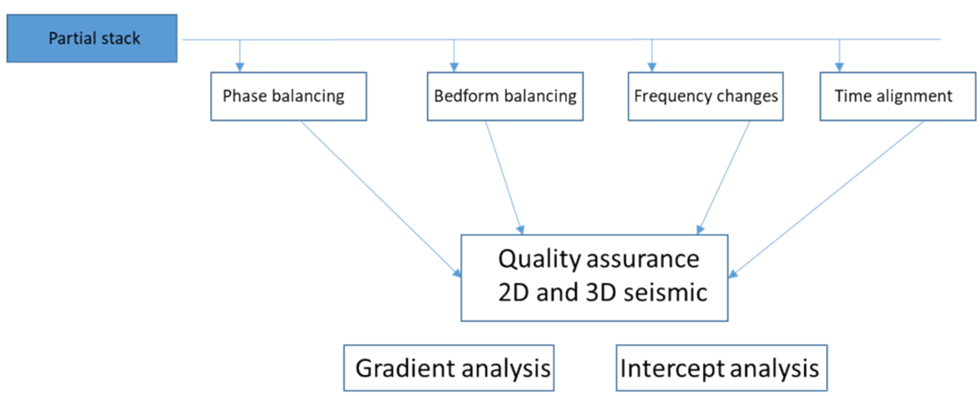

AVO analysis:

Once the neat medium and far reflectivity dataset have been QC using the workflow procedure described above they are analysed with the target of calculating the gradient and intercept.

Gradient and intercept from partial stack are calculated using the following expressions:

Gradient: $= \frac{(R(\theta_f) - R(\theta_n)}{(Sin\theta_f^2 - Sin\theta_n^2)}$

Intercept:= $R(0) = R(\theta_n) - Gradient * (sin\theta_n^2)$

The angles θ_n and $\theta_f$represents the near and far angle stacks (in our case values are 5 and 15) and the values are plotted across gradient versus intercept volume.